



THE EFFECT OF MATERIAL INHOMOGENEITY ON THE FREE VIBRATIONS OF FGM CIRCULAR BEAMS

György Szeidl¹, László Péter Kiss²

^{1,2} Institute of Applied Mechanics, University of Miskolc, Miskolc, HUNGARY
gyorgy.szeidl@uni-miskolc.hu, mechkiss@uni-miskolc.hu

Abstract: Vibrations of heterogeneous curved beams have recently been investigated by the authors of the present paper. Various papers deal with, among others, the issue what effect the central load has on the vibrations of curved beams made of heterogeneous material with distinct supports. To find numerical solution, the authors determined the Green function matrices for pre-loaded beams. Then they reduced the eigenvalue problems, which yield the eigenfrequencies as a function of the load, to eigenvalue problems governed by a system of Fredholm integral equations. In this paper the most important properties of the model and the governing differential equations are provided for elastically restrained pre-loaded beams. Then the question how functionally graded material distribution can affect the eigenfrequencies is replied through examples.

Keywords: Curved beam, functionally graded material, natural frequency as a function of the load, Green function matrix

1. INTRODUCTION

Curved beams are widely used in engineering applications – let us consider, for instance, arch bridges or roof structures. Research concerning the mechanical behavior of such structural elements began in the 19th century. The free vibrations of curved beams have been under extensive investigation – see, e.g.: [1,2] for more details. Considering the vibrations of pre-loaded circular beams, the number of the available articles is much less than for the free vibrations. Wasserman [2], for example, investigates the load-frequency relationship for spring supported inextensible arches. The load can be dead or follower. Here, similarly as in [3], the Galerkin method was presented as an effective way to get solutions. Chidamparam and Leissa [3] investigate the vibrations of pinned-pinned and fixed-fixed pre-stressed homogeneous circular arches under distributed loads. The extensibility of the centerline is taken into account. In this paper we would like to discuss shortly a model which can be used to get the free and loaded vibrations of rotationally restrained nonhomogeneous circular beams. Through simple numerical examples, we show how functionally graded material (FGM) distribution can change the eigenfrequencies compared to homogeneous material distribution.

2. THE MECHANICAL MODEL

Here, based on [4] we overview the most important properties and assumptions used for the mechanical model. We have developed a 1D beam model to investigate the vibrations of the beam. The curvilinear coordinate system $(\xi = s, \eta, \zeta)$ is attached to the (E – weighted) centerline as shown in Figure 1. The radius of curvature ρ_0 is constant and, moreover, the cross-sectional geometry and the material distribution are uniform. However, the material composition and thus the material parameters are functions of the cross-sectional coordinates η, ζ and the axis ζ is a symmetry axis both for the geometry and for the material distribution. Therefore, it is possible to model homogeneous, functionally graded (FG) and even multi-layered beams, considering each material component to be linearly elastic and isotropic. At the points of the centerline, the E -weighted first moment of the cross-section with respect to the axis η is zero:

$$Q_{e\eta} = \int_A E(\eta, \zeta) \zeta dA = 0. \quad (1)$$

We consider the validity of the Euler-Bernoulli beam theory for the investigations, i.e., the cross-sections rotate as if they were rigid bodies and remain perpendicular to the deformed centerline. Let u_0 , w_0 and ϑ be the

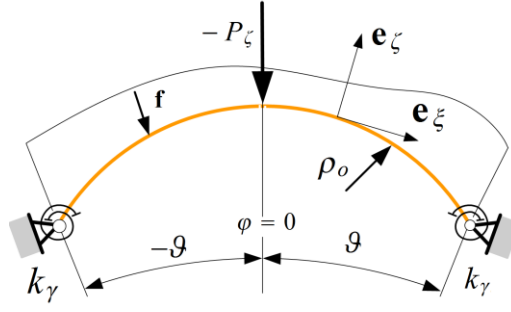


Figure 1: The beam centerline with loading and supports

tangential, radial displacements and the semi-vertex angle of the beam. Since the radius is constant the coordinate line s and the angle coordinate φ are related to each other via equation $s = \rho_o \varphi$. The axial strain $\varepsilon_{o\xi}$ and the rigid body rotation $\psi_{o\eta}$ on the centerline can be expressed [5] in terms of the displacements as

$$\varepsilon_{o\xi} = \frac{du_o}{ds} + \frac{w_o}{\rho_o}, \quad \psi_{o\eta} = \frac{u_o}{\rho_o} - \frac{dw_o}{ds}. \quad (2)$$

The principle of virtual work for the beam shown in Figure 1 yields equilibrium equations

$$\frac{dN}{ds} + \frac{1}{\rho_o} \left[\frac{dM}{ds} - \left(N + \frac{M}{\rho_o} \right) \psi_{o\eta} \right] + f_t = 0, \quad \frac{d}{ds} \left[\frac{dM}{ds} - \left(N + \frac{M}{\rho_o} \right) \psi_{o\eta} \right] - \frac{N}{\rho_o} + f_n = 0 \quad (3)$$

which should be fulfilled by the axial force N and the bending moment M . Here f_t and f_n denote the intensity of the distributed loads in the tangential and normal directions ($\mathbf{f} = f_t \mathbf{e}_\xi + f_n \mathbf{e}_\zeta$).

Recalling Hooke's law [1], the relations between the strains and inner forces become

$$N = \frac{I_{e\eta}}{\rho_o^2} \varepsilon_{o\xi} - \frac{M}{\rho_o}, \quad M = -I_{e\eta} \left(\frac{d^2 w_o}{ds^2} + \frac{w_o}{\rho_o^2} \right), \quad N + \frac{M}{\rho_o} = \frac{I_{e\eta}}{\rho_o^2} \varepsilon_{o\xi}, \quad \text{where} \quad (4)$$

$$A_e = \int_A E(\eta, \zeta) dA, \quad I_{e\eta} = \int_A E(\eta, \zeta) \zeta^2 dA, \quad m = \frac{A_e \rho_o^2}{I_{e\eta}} - 1.$$

A_e is the E -weighted area of the cross-section, $I_{e\eta}$ is the E -weighted moment of inertia with respect to the bending axis while m is a geometry-heterogeneity parameter – the effect of the material distribution is incorporated into the model through the latter one. For practical reasons, we introduce dimensionless displacements and a notational convention for the derivatives taken with respect to the angle coordinate:

$$U_o = \frac{u_o}{\rho_o}, \quad W_o = \frac{w_o}{\rho_o}; \quad (\dots)^{(n)} = \frac{d^n(\dots)}{d\varphi^n}, \quad n \in \mathbb{Z}. \quad (5)$$

If we plug equations (2) and (4) into (3) and perform some manipulations – these are detailed in [5] – we get

$$\begin{bmatrix} 0 & 0 \\ 0 & 1 \end{bmatrix} \begin{bmatrix} U_o \\ W_o \end{bmatrix}^{(4)} + \begin{bmatrix} -m & 0 \\ 0 & 2 - m\varepsilon_{o\xi} \end{bmatrix} \begin{bmatrix} U_o \\ W_o \end{bmatrix}^{(2)} + \begin{bmatrix} 0 & -m \\ m & 0 \end{bmatrix} \begin{bmatrix} U_o \\ W_o \end{bmatrix}^{(1)} + \begin{bmatrix} 0 & 0 \\ 0 & 1 + m(1 - \varepsilon_{o\xi}) \end{bmatrix} \begin{bmatrix} U_o \\ W_o \end{bmatrix} = \frac{\rho_o^3}{I_{e\eta}} \begin{bmatrix} f_t \\ f_n \end{bmatrix}. \quad (6)$$

Within the framework of the linear theory, we can freely neglect the effect of the deformations on the equilibrium (i.e., $\varepsilon_{o\xi} = 0$).

In the sequel, the increments (which occur because of the vibratory nature of the problem) in the typical quantities are identified by a subscript b . Each physical quantity can be given in a form similar to the total tangential displacement which is equal to the sum $u_o + u_{ob}$. Here u_o is the static displacement caused by the pre-load, and u_{ob} is the dynamic displacement increment. It turns out [4] that the increments in the axial strain and in the rotation have a similar structure to equations (2):

$$\varepsilon_{o\xi b} = \varepsilon_{o\xi b} + \psi_{o\eta} \psi_{o\eta b} \approx \varepsilon_{o\xi b}, \quad \psi_{o\eta b} = \frac{u_{ob}}{\rho_o} - \frac{dw_{ob}}{ds}, \quad \varepsilon_{o\xi b} = \frac{du_{ob}}{ds} + \frac{w_{ob}}{\rho_o}. \quad (7)$$

The principle of virtual work for the increments yields the equilibrium equations – see [2] for details:

$$\begin{aligned} \frac{d}{ds} \left(N_b + \frac{M_b}{\rho_o} \right) - \frac{1}{\rho_o} \left(N + \frac{M}{\rho_o} \right) \Psi_{onb} + f_{tb} &= 0, \\ \frac{d^2 M_b}{ds^2} - \frac{N_b}{\rho_o} - \frac{d}{ds} \left[\left(N + \frac{M}{\rho_o} \right) \Psi_{onb} + \left(N_b + \frac{M_b}{\rho_o} \right) \Psi_{on} \right] + f_{nb} &= 0, \end{aligned} \quad (8)$$

where f_{tb} and f_{nb} are forces of inertia:

$$f_{tb} = -\rho_a A \frac{\partial^2 u_{ob}}{\partial t^2}, \quad f_{nb} = -\rho_a A \frac{\partial^2 w_{ob}}{\partial t^2}, \quad (9)$$

in which A as the area of the cross-section and ρ_a as the average density of the cross-section. The increments of the inner forces can be given in terms of the displacement increments via Hooke's law:

$$N_b = \frac{I_{en}}{\rho_o^2} m \varepsilon_{o\xi b} - \frac{M_b}{\rho_o}, \quad M_b = -I_{en} \left(\frac{d^2 w_{ob}}{ds^2} + \frac{w_{ob}}{\rho_o^2} \right), \quad N_b + \frac{M_b}{\rho_o} = \frac{I_{en}}{\rho_o^2} m \varepsilon_{o\xi b}. \quad (10)$$

Substituting (8) and (11) into (9), we get the equilibrium equations in the following form:

$$\begin{aligned} \begin{bmatrix} 0 & 0 \\ 0 & 1 \end{bmatrix} \begin{bmatrix} U_{ob} \\ W_{ob} \end{bmatrix}^{(4)} + \begin{bmatrix} -m & 0 \\ 0 & 2 - m \varepsilon_{o\xi} \end{bmatrix} \begin{bmatrix} U_{ob} \\ W_{ob} \end{bmatrix}^{(2)} + \\ + \begin{bmatrix} 0 & -m \\ m & 0 \end{bmatrix} \begin{bmatrix} U_{ob} \\ W_{ob} \end{bmatrix}^{(1)} + \begin{bmatrix} 0 & 0 \\ 0 & 1 + m(1 - \varepsilon_{o\xi}) \end{bmatrix} \begin{bmatrix} U_{ob} \\ W_{ob} \end{bmatrix} = \frac{\rho_o^3}{I_{en}} \begin{bmatrix} f_{tb} \\ f_{nb} \end{bmatrix}. \end{aligned} \quad (11)$$

As regards the details we refer the reader to [2]. For harmonic vibrations the amplitudes \hat{U}_{ob} and \hat{W}_{ob} should satisfy the following differential equations:

$$\begin{aligned} \mathbf{K}[\mathbf{y}(\varphi), m, \varepsilon_{o\xi}] = \begin{bmatrix} 0 & 0 \\ 0 & 1 \end{bmatrix} \begin{bmatrix} y_1 \\ y_2 \end{bmatrix}^{(4)} + \begin{bmatrix} -m & 0 \\ 0 & 2 - m \varepsilon_{o\xi} \end{bmatrix} \begin{bmatrix} y_1 \\ y_2 \end{bmatrix}^{(2)} + \begin{bmatrix} 0 & -m \\ m & 0 \end{bmatrix} \begin{bmatrix} y_1 \\ y_2 \end{bmatrix}^{(1)} + \\ + \begin{bmatrix} 0 & 0 \\ 0 & 1 + m(1 - \varepsilon_{o\xi}) \end{bmatrix} \begin{bmatrix} y_1 \\ y_2 \end{bmatrix} = \begin{bmatrix} r_1 \\ r_2 \end{bmatrix}; \quad \begin{bmatrix} y_1 \\ y_2 \end{bmatrix} = \begin{bmatrix} \hat{U}_{ob} \\ \hat{W}_{ob} \end{bmatrix}; \quad \begin{bmatrix} r_1 \\ r_2 \end{bmatrix} = \lambda \begin{bmatrix} \hat{U}_{ob} \\ \hat{W}_{ob} \end{bmatrix}; \quad \lambda = \rho_a A \frac{\rho_o^3}{I_{en}} \alpha^2, \end{aligned} \quad (12)$$

where λ and α denote the eigenvalues and eigenfrequencies.

This differential equation can be rewritten into the following form

$$\mathbf{K}[\mathbf{y}(\varphi), m, \varepsilon_{o\xi}] = \mathbf{r} \quad (13)$$

which, in fact, describes the behavior of the pre-loaded beam if the beam is subjected to a further dimensionless load \mathbf{r} .

For rotationally restrained beams differential equations (12) or (13) are associated with the following boundary conditions:

$$\hat{U}_{ob} \Big|_{\varphi=\pm\vartheta} = 0, \quad \hat{W}_{ob} \Big|_{\varphi=\pm\vartheta} = 0, \quad [\hat{W}_{ob}^{(2)} \pm \mathbf{K}_\gamma \hat{W}_{ob}^{(1)}] \Big|_{\varphi=\pm\vartheta} = 0 \quad (14)$$

where $\mathbf{K}_\gamma = k_\gamma \rho_o / I_{en}$ is a dimensionless spring constant given in terms of the spring constant k_γ . Equations (12) and (14) determine an eigenvalue problem. The i -th eigenfrequency α_i depends on the heterogeneity parameters m , ρ_a and also on the magnitude and the direction of the concentrated force P_ζ . The effect of the latter one is accounted through the axial strain it causes: $\varepsilon_{o\xi} = \varepsilon_{o\xi}(\mathbf{P}, m, \vartheta)$ in which \mathbf{P} is a dimensionless load:

$$\mathbf{P} = P_\zeta \rho_o^2 \vartheta / (2I_{en}).$$

It can be shown [4] that the Green function matrix can be constructed in closed-form for the above problem. With the Green function matrix, the eigenvalue problem can be transformed to a Fredholm integral equation system. Its kernel is the Green function matrix. Solution to the integral equations is possible with numerical methods as shown in [5].

3. NUMERICAL EXAMPLE ON THE FREE VIBRATIONS

In this section we illustrate how material inhomogeneity can affect the eigenfrequencies of pinned-pinned members, i.e., $\mathbf{K}_\gamma = 0$ and $P_\zeta = 0$. We consider a functionally graded material composition – see Figure 2, where C_c is the point where the centerline intersects the cross-section. The material properties, i. e., Young's

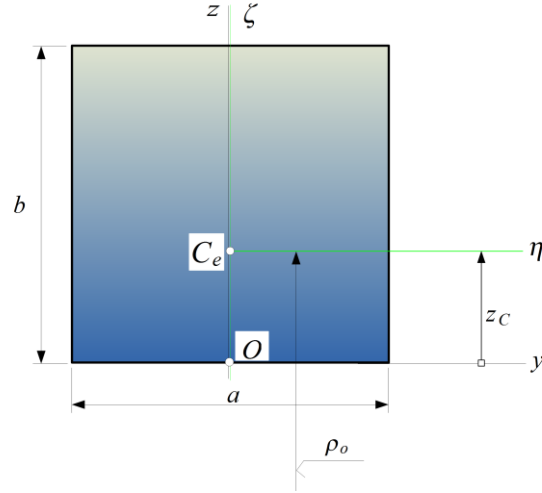


Figure 2: A functionally graded rectangular cross-section

modulus $E = E(\zeta)$ and the density ρ are distributed along the axis Z (or ζ) of the rectangular cross-section according to the power law rules:

$$E(z) = (E_m - E_c) \left(\frac{z}{b} \right)^k + E_c, \quad \rho(z) = (\rho_m - \rho_c) \left(\frac{z}{b} \right)^k + \rho_c. \quad (15)$$

Here the subscripts c and m refer to the ceramic and metal constituents of the material and the exhibitor $k \in \mathbf{R}$. In this example we choose an aluminium oxide Al_2O_3 and aluminium constitution, therefore

$$E_c = 38 \cdot 10^4 \text{ MPa}; \quad E_m = 7 \cdot 10^4 \text{ MPa}; \quad \rho_c = 3.8 \cdot 10^{-6} \frac{\text{kg}}{\text{mm}^2}; \quad \rho_m = 2.707 \cdot 10^{-6} \frac{\text{kg}}{\text{mm}^2}. \quad (16)$$

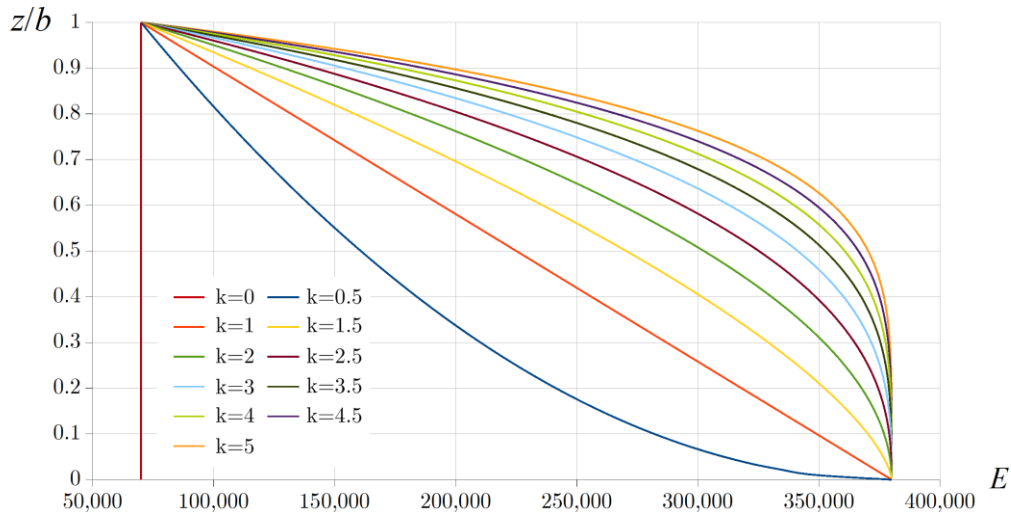


Figure 3: Variation of Young's modulus over the height of the cross-section

The value of the index k will be increased gradually from 0 by 0.5 until 5. If $k=0$, the cross-section is homogeneous aluminium and the typical quantities will be distinguished by a subscript $_{\text{hom}}$. Otherwise, the subscript $_{\text{het}}$ is used. (When $k \rightarrow \infty$ the whole cross-section is Al_2O_3 with a thin aluminium layer at $z = b$.) In Figure 3, we show the distribution of E along the height of the cross-section according to the power law. Next, we plot how the parameter m changes because of the inhomogeneity. Based on (4)₆ we have

$$\frac{m_{\text{het}}}{m_{\text{hom}}(k=0)} = \frac{A_c I_{e\eta}}{A I_{e\eta}} \left[\frac{\rho_{o \text{ het}}}{\rho_{o \text{ hom}}} \right]^2. \quad (17)$$

Recalling formulae (4)₄-(4)₅ and the data (16), the typical physical quantities we need to tackle the current problem can all be calculated. Therefore, the quotient (17) in terms of k and ρ_o/b is shown in Figure 4.

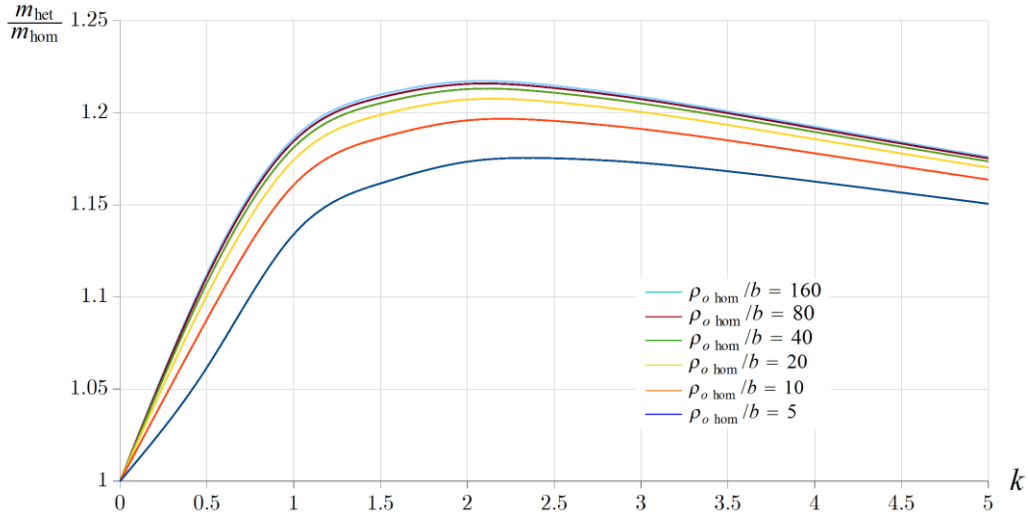


Figure 4: The quotient (17) against k and ρ_o/b

Now let us see how inhomogeneity can affect the first four natural frequencies of pinned-pinned circular beams. We choose $m_{hom} = 1200$ and $\rho_o/b = 10$, therefore the maximum of the quotient m_{het}/m_{hom} is 1.196 at $k = 2$. The selected semi-vertex angles are $\vartheta = (0.2; 0.4; 0.8; 1.6)$. The computational results are plotted in Figure 5 for $i=1,2,3,4$ – i.e., for the first four natural frequencies.

Generally we can conclude that there are significant differences because of the inhomogeneity. When $\vartheta = 0.2$, all four frequencies change in a similar way and in the order from the first one to the fourth one. Interestingly, when $\vartheta = 0.4$, only the second, third and fourth frequencies change almost exactly the same way. Increasing the semi-vertex angle to 0.8, we again experience a new tendency: the even frequencies are affected mostly by the material composition. On the bottom right diagram the curves coincide with a good accuracy.

We have also carried out some simple finite element computations to verify our model. We have used the following data: $a = b = 10\text{mm}$, $\rho_o/b = 30$, and the material was aluminium ($k = 0$ - see the material properties beforehand). In the commercial finite element software Abaqus CAE 6.7 we have combined the Static, General and the Linear Perturbation, Frequency steps with B22 beam elements. Some simple comparisons for $\vartheta = 0.2; 0.5; 1$ are provided in Table 1. The table indicates that the models coincide really well for unloaded beams.

Table 1: Comparisons with finite element results

| ϑ | $\frac{\alpha_{1 \text{ New model}}}{\alpha_{1 \text{ Abaqus}}}$ | $\frac{\alpha_{2 \text{ New model}}}{\alpha_{2 \text{ Abaqus}}}$ | $\frac{\alpha_{3 \text{ New model}}}{\alpha_{3 \text{ Abaqus}}}$ | $\frac{\alpha_{4 \text{ New model}}}{\alpha_{4 \text{ Abaqus}}}$ |
|-------------|--|--|--|--|
| 0.2 | 1.001 | 1.037 | 1.079 | 1.213 |
| 0.5 | 1.006 | 1.010 | 1.004 | 1.025 |
| 1 | 1.002 | 1.004 | 0.996 | 1.011 |

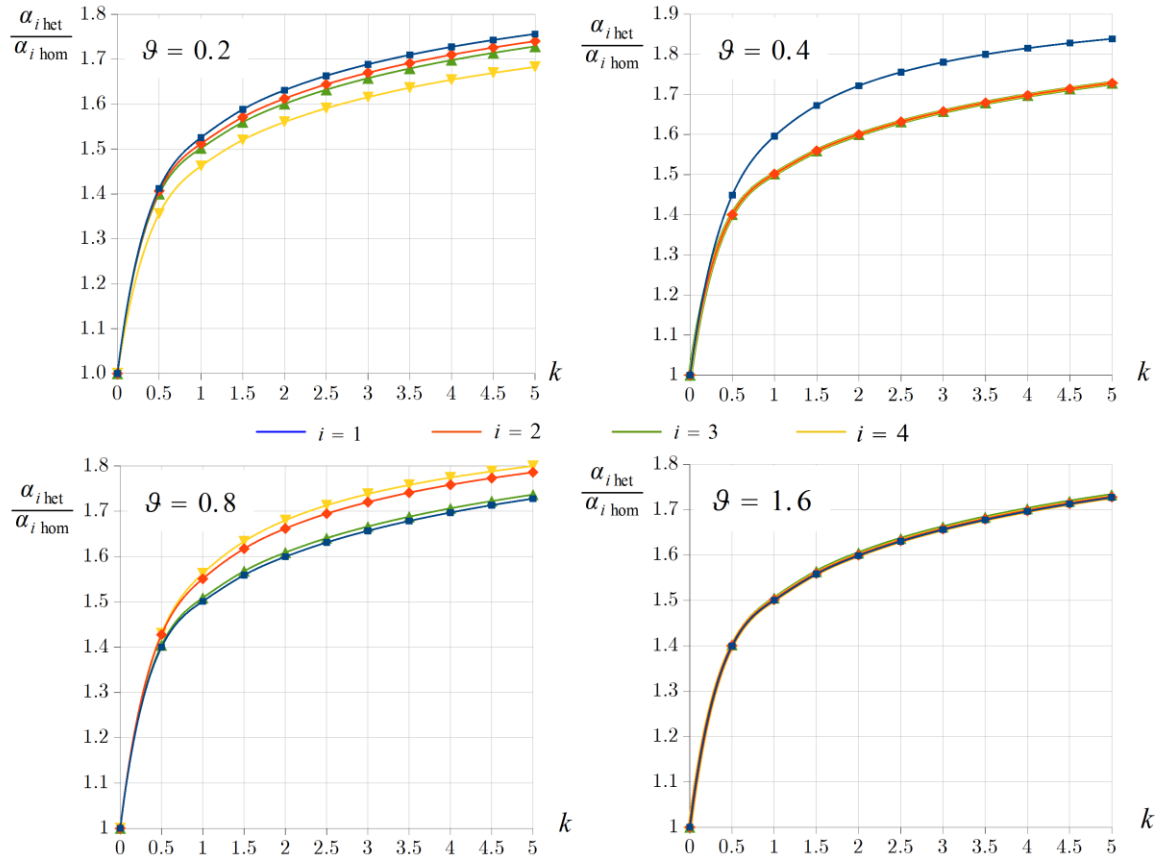


Figure 5: The change in the frequencies due to the inhomogeneity

4. CONCLUSIONS

We have presented a model to clarify the vibratory behavior of circular beams pre-loaded by central load (a vertical force at the crown point). The model is based on the Euler-Bernoulli beam theory and is applicable for heterogeneous materials. The beam-end supports are rotationally restrained pins, which are modeled by linear volute springs having the same spring constant. The effect of the pre-load is incorporated into the model via the strain it causes. An eigenvalue problem was established by using the principle of virtual work. This eigenvalue problem can be transformed to an eigenvalue problem governed by Fredholm integral equations similarly as in [4]. The Green function matrix can also be given in a closed form both for compressive load and for tensile load. Through simple numerical examples, we showed that functionally graded material distribution can significantly change the eigenfrequencies compared to homogeneous material distribution.

Acknowledgements: This research was supported by the National Research, Development and Innovation Office - NKFIH, K115701.

REFERENCES

- [1] Gy. Szeidl. *The Effect of Change in Length on the Natural Frequencies and Stability of Circular Beams*. Ph.D. thesis. Department of Mechanics, University of Miskolc, Hungary, 1975. (in Hungarian)
- [2] Y. Wasserman. The Influence on the Behavior of the Load on the Frequencies and Critical Loads of Arches with Flexibly Supported Ends. *Journal of Sound and Vibration*. 54(4):515-526, 1977.
- [3] P. Chidamparam, A. W. Leissa. Influence of Centerline Extensibility on the In-plane Free Vibrations of Loaded Circular Arches. *Journal of Sound and Vibration*. 183(5):779-795, 1995.
- [4] L. P. Kiss, Gy. Szeidl. Vibrations of Pinned-fixed Heterogeneous Circular Beams Pre-loaded by a Vertical Force at the Crown point. *Journal of Sound and Vibration* 393:92-113, 2017.
- [5] L. P. Kiss. *Vibrations and Stability of Heterogeneous Curved Beams*. Ph.D. thesis. Institute of Applied Mechanics, University of Miskolc, Hungary. 2015. pp. 142.